Scientific Research Publishing

Open Journal of Applied Sciences, 2023, 13, 2320-2328
https://www.scirp.org/journal/ojapps
ISSN Online: 2165-3925
ISSN Print: 2165-3917

Dual-System Activation of Ni-Base Superalloy under High Strain and High Temperature

Alexandru Lopazan, Alberto W. Mello*

Embry-Riddle Aeronautical University, Daytona Beach, FL, USA
Email: *melloa2@erau.edu

How to cite this paper: Lopazan, A. and Mello, A.W. (2023) Dual-System Activation of Ni-Base Superalloy under High Strain and High Temperature. *Open Journal of Applied Sciences*, **13**, 2320-2328.
https://doi.org/10.4236/ojapps.2023.1312181

Received: November 21, 2023
Accepted: December 15, 2023
Published: December 18, 2023

Abstract

Due to their superior combination of heat resistance, high temperature corrosion resistance, toughness and strength, nickel-based superalloys have become of extensive use in the aerospace industry. This research aims to explain why the fatigue life of Inconel-718 in preconditioned samples had larger fatigue lives than pristine samples. The hypothesis is that preconditioning at 700˚C and 1.0% strain could lead to thermal activation of the {100} cubic slip plane alongside the {111} octahedral slip plane, potentially improving fatigue life. Using SEM and EBSD imaging, the microstructure of Inconel-718 samples were characterized before and after preconditioning. The directions of the slip bands that formed following the preconditioning were determined. The result was that the existence of both the cubic and octahedral slip systems was confirmed, leading to the thermal activation hypothesized. The existence of both slip planes was considered to be the reason behind the improved fatigue life due to better strain accommodation within the microstructure. It is suggested that focuses for future research includes conducting *in-situ* observation of slip activation and the application of preconditioning as a manufacturing method.

Keywords

Metal Fatigue, Ni-Based Superalloys, Cube Slip, Microstructure, High Temperature

1. Introduction

As propulsion technology in the aviation industry began to become more advanced, the needs for a material that was able to counter restricting factors such as high temperature operation, creep, and vibrational loads increase [1]. Previously, studying of new materials and combination of different metals around

1930 lead to the discovery of the γ' phase. This is the primary strengthening phase for nickel-based superalloys. Later, the γ'' phase was found specifically in Inconel-718 [2]. Superalloy microstructure is characterized by different solid phases that each has a unique effect on the superalloy's mechanical properties. Some examples of these solid phases include the matrix γ, Carbides (MC, M6C, M23C6), Laves, μ, σ, and the previously mentioned strengthening phases [3]. The main characteristics that make superalloys desirable include their high toughness, resistance to corrosion, resistance to creep, and resistance to high temperature. In general, superalloys are ideal for operating at temperatures at or above 500˚C with their upper temperature tolerance reaching as high as 1200˚C, about 70% of their melting temperature. These properties overall made nickel-based superalloys excellent for usage in aircraft and rocket propulsion systems [4]. At this point, superalloys account for roughly 50% of the total weight of aircraft engines. Inconel-718 particularly comprises about 34% of the superalloys used and is primarily found in combustor and turbine regions. Other areas that use superalloys include engine shafts, afterburners, thrust reversers, etc. [5]. One topic that is important to superalloy study is material fatigue. In general, stress levels in cyclic loading tend to be considerably lower than the ultimate load value of the material. It is rare for a structure, particularly in aircraft, to fail due to operational loading exceeding the material ultimate load. The reason why fatigue has a large role in aircraft is due to their naturally cyclic operation. The danger that fatigue poses to a structure is that it directly causes material failure. Failure due to fatigue occurs in three stages: nucleation, initiation, and propagation [6]. It has been well established that strain localization at material tends to cause origin points for cracking. The risk of crack formation and reaching critical size causing failure is always present and must be understood and accounted for [7]. The strain localization under cyclic loading is formed by dislocation motion during plastic deformation and it is concentrated in slip bands within the grains. In general, the direction of the lip bands is characterized by slip systems within the microstructure.

The study of fatigue effects and how they specifically interact in nickel-based superalloys is a subject of current studies. The effects of microstructure, environment, applied loading, and manufacturing methods on fatigue severity, crack modeling, and fatigue life are important to be understood for safe operation of a structure. The influence that dislocations have on fatigue severity is dependent on material particle size and grain orientation [8] [9]. It was found that alloying and having larger particle size within the material leads to the restriction of dislocation slip, leading to improved fatigue life. Using dislocation effects to model crack growth was proved to be an effective method and reinforced the importance of slip systems have on fatigue [10]. The effects of microstructure on fatigue of nickel-based superalloys heavily depend on crystal size and orientation [11] [12]. Conducting Low Cycle Fatigue (LCF), High Cycle Fatigue (HCF), and other environmental based tests have helped characterize the effects of dislocations and other microstructure characteristics on the fatigue of a material. To

successfully observe the evolution of the dislocations following fatigue testing, these studies primarily made use of SEM, DIC, and EBSD imaging of the material microstructure. Much research has been focused on what EBSD techniques can be used to better observe and characterize material microstructures focusing on superalloys and other materials [13] [14]. Observations of activated slip system trace angles, slip bands, crystallographic orientations, and other characteristics are able to be used to characterize strain localization, which is a precursor to fatigue effects. Overall, literature involving fatigue testing and fatigue characteristics is extensive and the focus of Ni-based superalloy fatigue is growing.

Ni-based superalloys do not exhibit a significant decrease in the yield strength between room temperature and 700˚C. This anomalous phenomenon is not common among engineering alloys. In addition, the strength may increase over this range of temperatures, what makes superalloy suitable for high temperature environment operation. One explanation for this characteristics is a cross-slip mechanism of the dislocations from the octahedral {111} planes to the cubic {100} planes. Studies of this strengthening behavior have been recently extended to fatigue lives of samples submitted to cross slip mechanism. The present work aims to corroborate the hypothesis of Mello *et al.* [7] and De La Torre and Mello [15] that dual-system activation happens under high strain and high temperature. In the first cited work, fatigue testing and strain mapping of the RR1000 Ni-based superalloy at various temperatures, cycle numbers, and applied strain showed improved strain accommodation at 700˚C and 1.0% strain. It was theorized that this case resulted in favorable thermal activation of the {100}, and this could lead to improved fatigue life [7]. This potential improvement in fatigue life was confirmed by fatigue testing of Inconel 718 samples. Based on the previously mentioned findings, IN-718 samples were "preconditioned" at 700˚C at 1.0% before conducting standard fatigue testing. The fatigue lives of unconditioned IN-718 were compared to preconditioned samples and the result was a fatigue life of preconditioned samples four times greater than normal samples [15]. The main purpose of the present research is to confirm that the cause of fatigue life increase of IN-718 by the later research had the same cause as the one hypothesized by the previous study of the proprietary RR1000. Scanning Electron Microscope (SEM) and Electron Backscattered Diffraction (EBSD) were used to characterize the microstructure of IN-718 before and after preconditioning to confirm thermal activation of {100} slip plane resulting in improved fatigue life.

2. Methodology

The experimentation process of this research involved material preparation stage, largely following the sample preparation process of previous work of De La Torre and Mello [15]; and the microstructure characterization using SEM and EBSD before and after material preconditioning at 700˚C and 1.0% strain stage.

2.1. Equipment

The following equipment sets were used in this research. For sample prepara-

tion, Buehler Metaserv 250 Twin Polisher, Pace Technologies GIGA-1200 Vibratory Polisher, Branson Ultrasonic Cleaner, and Wilson Tukon 1202 Micro-Hardness Tester. For mechanical loads and thermal experiments MTS Model 204.61 Servo Hydraulic System, MTS Controller, ATS Series 3430 Split Furnace, and an ATS P-20-115 Temperature Controller. For Microstructure characterization, FEI Quanta 650 Scanning Electron Microscope, Bruker Quantax 400 Electron Backscatter Diffraction (Figure 1).

2.2. Procedure

The procedures for the sample preparation phase involve polishing, cleaning, and marking the IN-718 samples so that SEM and EBSD imaging can be conducted. The following process was used for polishing: 600 grit followed by 1200 grit polishing on the twin polisher until a mirror like finish was achieved and then finished by leaving the sample 24 hours in the vibratory polisher using Nappad and 0.05 μm colloidal silica. Samples were placed in individual vials with varying chemicals and sonicated using the ultrasonic cleaner for a certain amount of time. The following protocol and chemicals were used: acetone for 5 minutes, isopropyl alcohol (IPA) for 10 minutes, and methanol for 5 minutes. This process was repeated before the samples were placed in the SEM chamber. The final step for sample preparation was delimiting an area of interest (AOI) on the surface of each sample using the Wilson Tuker's indenter function. The purpose is to have a distinct area to observe the changes in the microstructure before and after preconditioning. Figure 2 shows a diagram of the indentation marks, their positions, orientation, relative size, and force applied to generate them.

The procedure for preconditioning involved using the MTS frame and ATS furnace to apply a 1.0% strain at 700˚C on each sample. Each sample was loaded into the frame and the furnace was closed around it. The furnace temperature

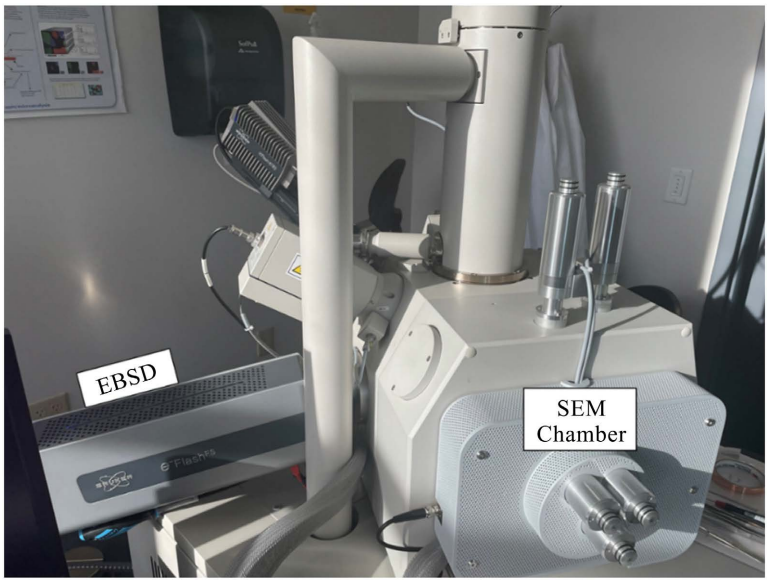

Figure 1. Bruker EBSD and SEM used for experimentation.

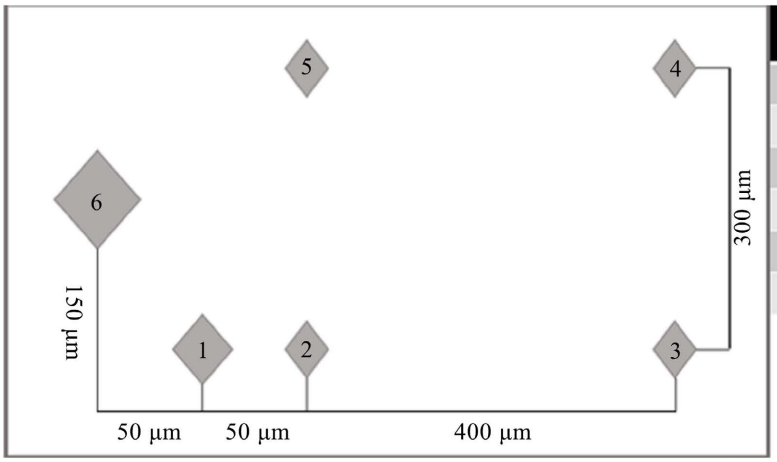

Indent	Force (grams)
1	50
2	25
3	25
4	25
5	25
6	200

Figure 2. Area of Interest (AOI) diagram with indent sizes and applied force.

was slowly increased by intervals that reduced as the target temperature was approached to avoid overshoot and potentially overheating the sample. After each interval, the sample was given a few seconds to settle at the temperature and this was repeated until reaching 700˚C. Once the temperature was achieved, the samples were slowly loaded along its x direction to a force that corresponded to a 1.0% strain. The applied strain was reached, and the samples were held at that force for 1 minute to allow the microstructure to settle. The samples were then unloaded and allowed to return to room temperature before being removed. For SEM imaging and EBSD analysis, the samples were cleaned with the same method discussed in the sample preparation stage. The samples were then mounted on aluminum holders using carbon tape and extra copper tape for better grounding. A flat aluminum holder was for SEM topography, and a 45˚ holder was used for EBSD analysis. The SEM stage was then tilted by 25˚, making a 70˚ tilt so the specimens are properly oriented for the Bruker Quantax 400 EBSD analysis.

3. Results

Prior to pre-conditioning, the samples were indented and marked as explained before. Then a full EBSD mapping was conducted over the AOI, as shown in Figure 3. This figure shows the Inverse Pole Figure (IPF-z) and the crystallography orientation map of one sample's AOI. Before loading the samples under heat, their dimensions were confirmed for further stress calculation. Figure 4 shows one of the samples after loading the specimen to 1% strain under 700˚C. Following the preconditioning the samples, the specimens were observed in the SEM for slip activity mapping. Figure 5 shows an example of clear grains' highlights and slip bands formed within the grains.

Using the SEM images and EBSD crystallographic orientation determined before preconditioning, we could map the slip planes' activations. Figure 4 brings a comparison between a polished sample, Figure 4(b), and the AOI after loading, Figure 4(c). Figure 5(a) just depicts a dimension comparison between a

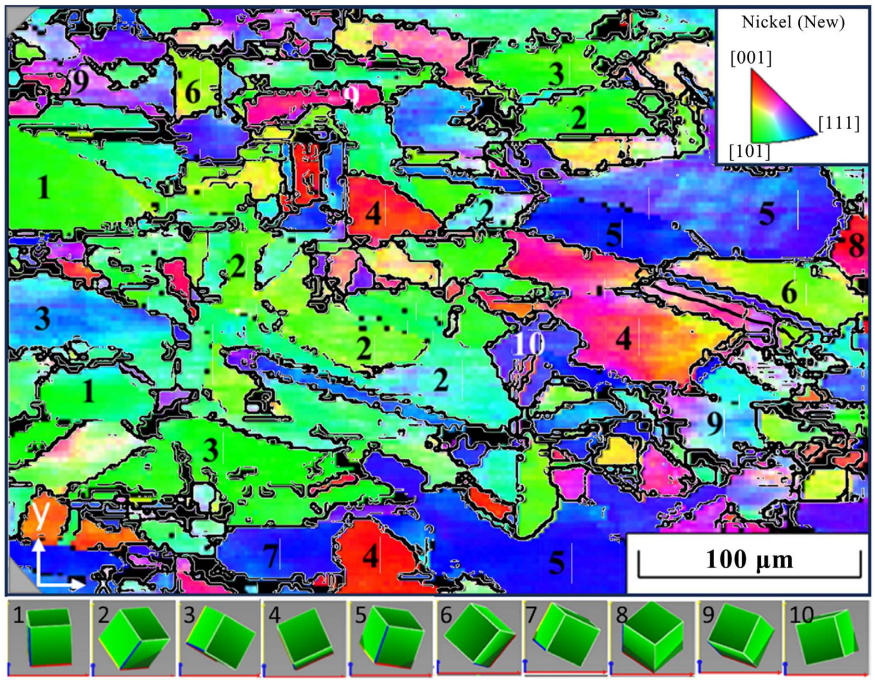

Figure 3. IPF-z and crystallographic orientations of sample #2.

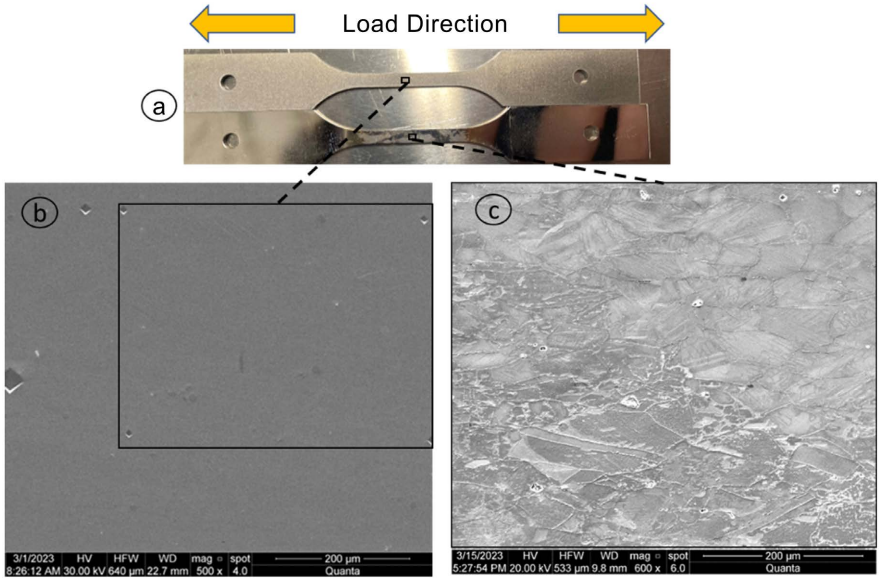

Figure 4. Sample 2 following preconditioning compared to a standard sample (a). SEM image of polished sample (b), SEM image after preconditioning (c).

pristine and pre-strained sample. Following the capture of all necessary images before and after preconditioning, the first step to conduct the comparison was to find an equivalency between the grains in the EBSD maps and the visible grains in the SEM images following preconditioning.

Figure 5 brings an example of equivalency mapping for a few identified slip directions of one sample. Finding this equivalency meant that each grain can be studied to compare the original crystallography orientation defined by EBSD

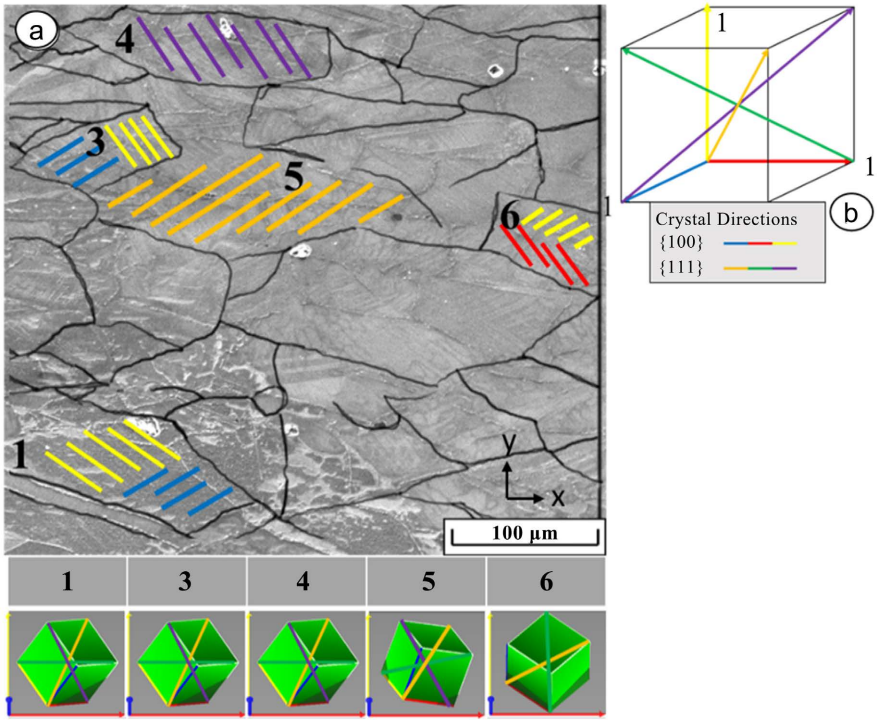

Figure 5. Slip band directions characterized by original crystal orientation for Sample 2.

mapping. As seen in Figure 5(a) for sample 2, grains 1, 3, and 6 have two distinct slip band directions while grains 4 and 5 only have one slip band direction. After matching with the IPF shown in Figure 3, considering the crystal directions exemplified in Figure 5(b), the slip bands can be categorized based on the original crystallography orientation of the grains.

Analyzing Figure 5 we concluded that grains 4 and 5 were defined by crystal orientations in the {111} directions. The bidirectional slip bands of grains 1, 3, and 6 were defined by crystal orientations in the {100} directions.

4. Discussion

The results of preconditioning of IN-718 coupons to 1% strain at 700C showed the same results previously found for the proprietary RR1000 in a previous research. The samples were closely monitored during loading to avoid any negative effect on the results. The grains of the sample before pre-loading were mapped and characterized by their initial crystal orientation inside an AOI. After successfully drawing an equivalency between the grains before and after the loading, the slip systems of the grains were determined. Upon analysis of the SEM images and EBSD mappings, we observed that a few grains displayed only one slip band direction, while a few others had activated two directions. Comparing them to their respective crystal orientation, it became clear that both the {111} and {100} slip system were activated in the observed scale. However, it is important to consider, as theorized by Bettge and Österle [16], that the mesoscale cubic slip plane activity may be following the zig-zag mechanism in the matrix, then the result

observed in the SEM resolved scale is an overall slip along the cubic slip system. To clarify this point, a TEM investigation with dislocations cross-slip between {111} planes in the γ matrix and shear the γ' precipitates about the {100} planes in a polycrystalline Ni-based superalloy should be investigated as performed by Philips *et al.* [17] for their R104, under fatigue loading.

5. Conclusions

Based on the resulting characterization of the slip band directions in both the {111} and {100} direction, the cubic slip system was indeed thermally activated by the preconditioning process. The existence of both cubic and octahedral slip systems likely leads to reduced strain localization as the microstructure has changed in a favorable direction that better accommodates the stress. This can explain the findings of previous research and support the hypothesis that overload and high strain is a method that can improve the fatigue life of IN-718.

The recommendation of the authors is to conduct in-situ experimentation to observe the change in microstructure as the IN-718 specimens undergo preconditioning and conduct further study of preconditioning as a manufacturing method to produce parts with improved fatigue life.

Conflicts of Interest

The authors declare no conflicts of interest regarding the publication of this paper.

References

[1] Boyer, R.R., Cotton, J.D., Mohaghegh, M., *et al.* (2015) Materials Considerations for Aerospace Applications. *MRS Bulletin*, **40**, 1055-1066. https://doi.org/10.1557/mrs.2015.278

[2] Sims, C.T. (1984) A History of Superalloy Metallurgy for Superalloy Metallurgists. *Superalloys*, **1**, 399-419. https://doi.org/10.7449/1984/Superalloys_1984_399_419

[3] Antolovich, S.D. (2015) Microstructural Aspects of Fatigue in Ni-Base Superalloys. The Royal Society Publishing, London, 1-36. https://doi.org/10.1098/rsta.2014.0128

[4] Walley, J.L. (2013) Exploration of Local Strain Accumulation in Nickle-Based Superalloys. Graduate Program in Materials Science and Engineering, Ohio State University.

[5] Pollock, T.M. and Tin, S. (2006) Nickel-Based Superalloys for Advanced Turbine Engines: Chemistry, Microstructure, and Properties. *Journal of Propulsion and Power*, **22**, 361-374. https://doi.org/10.2514/1.18239

[6] Dowling, N.E. (1998) Mechanical Behavior of Materials: Engineering Methods for Deformation, Fracture, and Fatigue. 2nd Edition, Pearson, London.

[7] Mello, A.W., Nicholas, A. and Sangid, M. (2017) Fatigue Strain Mapping via Digital Image Correlation for Ni-Based Superalloys: The Role of Thermal Activation on Cube Slip. *Materials Science & Engineering: A*, **695**, 332-341. https://doi.org/10.1016/j.msea.2017.04.002

[8] Zhang, Z.J., An, X.H., Zhang, P., Yang, M.X., Yang, G., Wu, S.D. and Zhang, Z.F.

(2013) Effects of Dislocation Slip Mode on High-Cycle Fatigue Behaviors of Ultra-fine-Grained Cu-Zn Alloy Processed by Equal-Channel Angular Pressing. *Scripta Materialia*, **68**, 389-392. https://doi.org/10.1016/j.scriptamat.2012.10.036

[9] Watanabe, C., Monzen, R. and Tazaki, K. (2008) Effects of AL3Sc Particle Size and Precipitate-Free Zones on Fatigue Behavior and Dislocation Structure of an Aged Al-Mg-Sc Alloy. *International Journal of Fatigue*, **30**, 635-641. https://doi.org/10.1016/j.ijfatigue.2007.05.010

[10] Hansson, P. and Melin, S. (2005) Dislocation-Based Modelling of the Growth of a Microstructurally Short Crack by Single Shear Due to Fatigue Loading. *International Journal of Fatigue*, **27**, 347-356. https://doi.org/10.1016/j.ijfatigue.2004.09.002

[11] Larrouy, B., Villechaise, P., Cormier, J. and Berteaux, O. (2015) Grain Boundary-Slip Bands Interactions: Impact on the Fatigue Crack Initiation in a Polycrystalline Forged Ni-Based Superalloy. *Acta Materialia*, **99**, 325-336. https://doi.org/10.1016/j.actamat.2015.08.009

[12] Salvat Cantó, J., Winwood, S., Rhodes, K. and Birosca, S. (2018) A Study of Low Cycle Fatigue Life and Its Correlation with Microstructural Parameters in IN713C Nickel Based Superalloy. *Materials Science and Engineering*: *A*, **718**, 19-32. https://doi.org/10.1016/j.msea.2018.01.083

[13] Blochwitz, C., Brechbühl, J. and Tirschler, W. (1996) Analysis of Activated Slip Systems in Fatigue Nickel Polycrystals Using the EBSD-Technique in the Scanning Electron Microscope. *Materials Science and Engineering*: *A*, **201**, 42-47. https://doi.org/10.1016/0921-5093(95)10076-8

[14] Charpagne, M.A., Stinville, J.C., Callahan, P.G., Texier, D., Chen, Z., Villechaise, P., Valle, V. and Pollock, T.M. (2020) Automated and Quantitative Analysis of Plastic Strain Localization via Multi-Modal Data Recombination. *Materials Characterization*, **163**, Article ID: 110245. https://doi.org/10.1016/j.matchar.2020.110245

[15] De La Torre, P.E. and Mello, A.W. (2022) The Effect of Pre-Thermal and -Load Conditions on IN-718 High Temperature Fatigue Life. *Open Journal of Applied Sciences*, **12**, 406-419. https://doi.org/10.4236/ojapps.2022.123028

[16] Bettge, D. and Oesterle, W. (1999) Cube Slip in Near-[111] Oriented Specimens of a Single-Crystal Nickel-Base Superalloy. *Scripta Materialia*, **40**, 389-395. https://doi.org/10.1016/S1359-6462(98)00446-1

[17] Phillips, P.J., Unocic, R.R. and Mills, M.J. (2013) Low Cycle Fatigue of a Polycrystalline Ni-Based Superalloy: Deformation Substructure Analysis. *International Journal of Fatigue*, **57**, 50-57. https://doi.org/10.1016/j.ijfatigue.2012.11.008